Publication Year	2017
Acceptance in OA	2020-08-24T13:31:31Z
Title	Investigating the nature of the INTEGRAL gamma-ray bursts and sub-threshold triggers with Swift follow-up
Authors	Higgins, A. B., Starling, R. L. C., Götz, D., MEREGHETTI, Sandro, Wiersema, K., Maccarone, T., Osborne, J. P., Tanvir, N. R., O'Brien, P. T., Bird, A. J., Rowlinson, A., Gehrels, N.
Publisher's version (DOI)	10.1093/mnras/stx1163
Handle	http://hdl.handle.net/20.500.12386/26774
Journal	MONTHLY NOTICES OF THE ROYAL ASTRONOMICAL SOCIETY
Volume	470

Monthly Notices
of the
ROYAL ASTRONOMICAL SOCIETY

MNRAS **470,** 314–323 (2017)
Advance Access publication 2017 May 12

doi:10.1093/mnras/stx1163

Investigating the nature of the *INTEGRAL* gamma-ray bursts and sub-threshold triggers with *Swift* follow-up

A. B. Higgins,[1★] R. L. C. Starling,[1] D. Götz,[2] S. Mereghetti,[3] K. Wiersema,[1] T. Maccarone,[4] J. P. Osborne,[1] N. R. Tanvir,[1] P. T. O'Brien,[1] A. J. Bird,[5] A. Rowlinson[6,7] and N. Gehrels[8]

[1] *Department of Physics and Astronomy, University of Leicester, University Road, Leicester LE1 7RH, UK*
[2] *AIM-CEA/DRF/Irfu/Service d'Astrophysique, Orme des Merisiers, F-91191 Gif-sur-Yvette, France.*
[3] *INAF, IASF-Milano, via E.Bassini 15, I-20133 Milano, Italy.*
[4] *Department of Physics and Astronomy, Texas Tech University, Box 41051, Lubbock, TX 79409, USA*
[5] *School of Physics and Astronomy, University of Southampton, Southampton SO17 1BJ, UK*
[6] *Netherlands Institute for Radio Astronomy (ASTRON), PO Box 2, NL-7990 AA Dwingeloo, the Netherlands*
[7] *Anton Pannekoek Institute, University of Amsterdam, Postbus 94249, NL-1090 GE, Amsterdam, the Netherlands*
[8] *NASA Goddard Space Flight Center, Greenbelt, MD 20771, USA*

Accepted 2017 May 10. Received 2017 May 10; in original form 2016 December 16

ABSTRACT

We explore the potential of the *INTErnational Gamma-Ray Astrophysics Laboratory (INTEGRAL)* to improve our understanding of the low-fluence regime for explosive transients, such as Gamma-ray Bursts (GRBs). We probe the nature of the so-called 'WEAK' *INTEGRAL* triggers, when the gamma-ray instruments record intensity spikes that are below the usual STRONG significance thresholds. In a targeted *Swift* follow-up campaign, we observed 15 WEAK triggers. We find six of these can be classified as GRBs. This includes GRB 150305A, a GRB discovered from our campaign alone. We also identified a source coincident with one trigger, IGRW 151019, as a candidate active galactic nucleus. We show that real events such as GRBs exist within the INTEGRAL Burst Alert System (IBAS) WEAK trigger population. A comparison of the fluence distributions of the full *INTEGRAL* IBAS and *Swift*-BAT GRB samples showed that the two are similar. We also find correlations between the prompt gamma-ray and X-ray properties of the two samples, supporting previous investigations. We find that both satellites reach similar, low fluence levels regularly, although *Swift* is more sensitive to short, low-fluence GRBs.

Key words: gamma-ray burst: general.

1 INTRODUCTION

GRBs are among the most luminous events in the universe, releasing energies $>10^{51}$ erg typically in time periods of seconds (Gehrels & Mészáros 2012). During these events a huge amount of gravitational energy is released from a central engine, which leads to the formation of jets where particles are accelerated to ultrarelativistic speeds (Woosley & Heger 2006). Internal shocks within the jet produce the high-energy prompt gamma-ray emission, we first observe (Gehrels & Mészáros 2012; Piran 2003). The jet then shocks with the surrounding medium producing broad-band afterglow emission (Mészáros & Rees 1997; Wijers, Rees & Meszaros 1997). Classically, GRBs are split into two sub-groups based on their T_{90} – the duration over which 90 per cent of the gamma-ray flux is received (Kouveliotou et al. 1993). The two groups are short GRBs where $T_{90} < 2$ s and long GRBs where $T_{90} > 2$ s, linked with two different progenitor models.

GRBs span a large range of isotropic equivalent luminosities: $10^{45} \leq L_{\rm ISO} \leq 10^{54}$ erg s^{-1}. Investigations into their luminosity function and formation rates coupled with observations of several local GRBs (Sazonov, Lutovinov & Sunyaev 2004; Soderberg et al. 2004) have suggested that there should be a large number of low-luminosity GRBs (Daigne & Mochkovitch 2007; Liang et al. 2007; Pescalli et al. 2016). There are further suggestions that these could exist as a separate local population (Norris 2002; Norris et al. 2005; Chapman et al. 2007; Liang et al. 2007). We use two currently active GRB detecting missions, *Swift* (Gehrels et al. 2004) and The INTErnational Gamma-Ray Astrophysics Laboratory (*INTEGRAL*; Winkler et al. 2003), to look at potentially faint GRBs.

INTEGRAL carries two gamma-ray instruments, the imager - IBIS (Ubertini et al. 2003) and the spectrometer - SPI (Vedrenne et al. 2003). Alerts for GRBs and other transient sources are communicated with low latency by IBAS[1] (*INTEGRAL* Burst Alert

★ E-mail: abh13@le.ac.uk

[1] http://ibas.iasf-milano.inaf.it/

System; Mereghetti et al. 2003) discussed in more detail in Section 2. Since the launch in 2002, *INTEGRAL* has detected over 900 soft gamma-ray sources[2] (Bird et al. 2016) and has localized 114 GRBs (numbers correct as of 2016 July 1). *INTEGRAL* has made some important discoveries regarding GRBs, reviewed in Götz (2012), including investigations utilizing IBIS and SPIs capability to perform spectral analysis on the *INTEGRAL* sample of GRBs (Vianello, Götz & Mereghetti 2009; Bošnjak et al. 2014). Furthermore, Foley et al. (2008) suggested that *INTEGRAL* may be capable of detecting the local, low-luminosity GRB populations.

In the fully coded field of view (FOV), i.e. the central 9×9 deg^2, the *INTEGRAL* IBIS instrument is more sensitive than the Burst Alert Telescope (BAT; Barthelmy 2004) on board *Swift*, despite its smaller effective area (2600 cm^2 compared to 5200 cm^2). This is due to the fact that, at the energies we are interested in (15–200 keV), the background is dominated by the Cosmic X-ray diffuse emission, which is proportional to the FOV (a factor of about ten smaller for IBIS than for BAT). Therefore, *INTEGRAL* should be able to reach lower peak flux limits, especially for GRBs with hard spectra, where peak energies $>$50 keV (Bošnjak et al. 2014). However, since *INTEGRAL* spends a large fraction of its observing time observing at low Galactic latitudes, its sensitivity is reduced by the additional background caused by bright Galactic sources and hard X-ray Galactic diffuse emission. It is only since the *INTEGRAL* sub-threshold trigger campaign began (see Section 2) that lower sensitivities have been routinely accessible through WEAK alerts.

Swift has two additional instruments: the X-Ray Telescope (XRT; Burrows et al. 2005) and the Ultraviolet/Optical Telescope (UVOT; Roming et al. 2005), and has the ability to slew towards a BAT-detected burst or pre-selected target. Therefore, it can complement *INTEGRAL* with rapid multiwavelength, follow-up measurements. Using observations from both satellites, we expect to uncover both the temporal behaviour and energetics of both the WEAK alerts and *INTEGRAL* GRB sample and characterize their properties.

We start by discussing IBAS in more detail and describe our chosen WEAK triggers in Section 2. Our *Swift* follow-up analysis is discussed in Section 3. These are then analysed in conjunction with the total IBAS GRB sample in Section 4 with some comparisons to the *Swift* GRB population. We conclude with our summary in Section 5.

2 *INTEGRAL* IBAS ALERTS

INTEGRAL was designed as a general purpose gamma-ray observatory, not specifically optimized for the study of GRBs. However, its good imaging capabilities over an FOV of $\approx 30 \times 30$ deg^2 (9×9 deg^2 fully coded and 19×19 deg^2 half-coded) and the continuous telemetry downlink (due to its high elliptical orbit with a period of 3 days) made it possible to search and localize GRBs on the ground in near real time. This is done with the IBAS (Mereghetti et al. 2003), software running at the ISDC (*INTEGRAL* Science Data Centre; Courvoisier et al. 2003) since the launch of *INTEGRAL* in 2002 October.

No GRB triggering algorithm is implemented on board the satellite. The data reach the ISDC typically within 20 s after they have been collected and are immediately fed into the IBAS software, which exploits several burst detection programs in parallel. When a burst (or any other new transient source) is detected inside the FOV of the IBIS instrument, its coordinates are automatically distributed through the internet by means of Alert Packets based on the User Datagram Protocol (UDP). Their coordinates derived by IBAS have a mean with 1σ uncertainty of 2.1($\pm$0.5) arcmin.

IBAS also searches for GRBs detected in the anticoincidence shield (ACS) of the SPI instrument, which provides a good sensitivity over nearly the whole sky, but without localization and spectral information (von Kienlin et al. 2003). The ACS light curves are used for GRB localizations by triangulation with other satellites of the IPN network (Cline et al. 1999). In this investigation, we will not discuss SPI ACS results.

The search for GRBs in the IBIS data uses two different kinds of programs: rate monitor and image monitor programs. Rate monitors look for excesses in the light curve of the whole detection plane, while image monitors search for excesses in the deconvolved images. Both use data from ISGRI (Lebrun et al. 2003), the lower energy detector of IBIS, which provides photon by photon data in the energy range of 15 keV–1 MeV. Several instances of the rate and image monitors run in parallel using different settings for integration time-scales and energy range. When one (or typically more) of the monitor programs triggers, an imaging analysis is performed on an optimally selected time interval in order to confirm the source presence and derive its significance.

Two significance threshold levels, labelled STRONG and WEAK, have been implemented in IBAS for what concerns the distribution of Alert Packets. The positions of new sources with significance above the STRONG threshold are immediately distributed with Alert Packets. These positions automatically derived by the IBAS software can be later refined by interactive analysis. Until 2011, Alert Packets for sources with significance above the WEAK threshold and below the STRONG were distributed in real time only to members of the IBAS Team, who, after interactive analysis could in some cases confirm the presence of a GRB and distribute its coordinates. However, in the majority of the cases it was not possible, based on the *INTEGRAL* data alone, to confirm the real astrophysical nature of these low significance events. Since 2011 January 26, all the Alert Packets corresponding to detections above the WEAK threshold have been automatically distributed in real time to the external users who wish to receive them.

Among the 114 confirmed GRBs detected by IBAS, 17 have been detected as sub-threshold WEAK alerts and 54 were observed with *Swift*, either through an independent autonomous BAT trigger and subsequent follow-up, or through ToO follow-up that was uploaded at a later time, and have available XRT data.

2.1 Selection of WEAK alerts and follow-up

There have been 402 *INTEGRAL* WEAK triggers, below 8σ significance, before 2016 July 1; six of which were promoted to STRONG triggers and were later confirmed as GRBs. Out of the other 396, we analysed 15 WEAK triggers. They consisted of the following:

(i) 11 triggers that did not have prompt *Swift* slews and were target of opportunity observations from our campaign. We named them IGRWYYMMDD prior to source-type identification, broadly following the GRB naming convention, see Table 1. These are termed as ‘our chosen ToOs’.

(ii) Two other WEAK *INTEGRAL* triggers with ToOs requested elsewhere and had XRT data, but were not related to our 11 chosen triggers, were analysed. These are termed as ‘candidate GRBs’.

[2] http://www.isdc.unige.ch/integral/

Table 1. Table containing the properties of the 15 WEAK triggers. The four triggers at the bottom are the four candidate GRBs with previous XRT observations and were not part of our selected ToOs. The trigger number, significance (σ), RA, Dec. and localization error (90 per cent confidence) were all taken from IBAS.

ToO name	*INTEGRAL* trigger number	IBAS detection significance (σ)	RA (°) (J2000)	Dec. (°) (J2000)	Localization error (arcmin)
IGRW 160610	7488/0	6.7	359.90	61.57	3.8
IGRW 151019	7277/0	7.0	292.82	31.14	3.5
IGRW 150903	7231/0	6.7	239.17	−33.81	3.6
IGRW 150610	7005/0	7.1	178.32	16.03	4.8
IGRW 150305	6905/0	7.6	269.79	−42.62	3.4
IGRW 140219	6467/0	6.7	204.10	−45.06	3.6
IGRW 130904	6931/0	6.7	256.88	−32.01	3.6
IGRW 110718	6323/0	6.8	256.78	40.05	3.6
IGRW 110608	6297/0	6.8	315.28	32.041	3.6
IGRW 110428	6169/0	7.2	320.27	−33.96	3.5
IGRW 110112	6127/0	7.4	10.56	64.41	2.6
IGRW 150831	7228/0	7.3	220.98	−25.65	3.4
IGRW 121212	6720/0	7.9	177.90	78.00	3.3
IGRW 100909	6060/0	7.7	73.95	54.65	2.0
IGRW 091111	–	7.2	137.81	−45.91	2.9

Table 2. *Swift* XRT ToO observations and candidate counterpart source detections. XRT position (90 per cent confidence), RA and Dec. were taken from UKSSDC. $T_{\rm START}$ refers to the time elapsed between the GRB/trigger occurring and the time when the *Swift* observation began and $T_{\rm STOP}$ refers to the time elapsed between the GRB occurring and the time when the final *Swift* observation finished. $T_{\rm EXP}$ is the total XRT exposure time.

ToO name	*Swift* Obs ID	XRT position error (arcsec)	RA (°) (J2000)	Dec. (°) (J2000)	$T_{\rm START}$ (s)	$T_{\rm STOP}$ (s)	$T_{\rm EXP}$ (s)
IGRW 151019	20558	2.5	292.7836	31.1319	9600	2810 017	14 938
GRB 150831A	653838	1.6	221.0243	−25.6351	82	38 575	11 828
IGRW 150305A	33663	3.5	269.7606	−42.6638	17838	735 268	908
GRB 121212A	541371	1.4	177.7923	78.0371	60	145 420	22 940
GRB 100909A	20147	3.3	73.9488	54.6579	11693	25 787	7720
GRB 091111	20120	7.7	137.8233	−45.9253	100360	197 466	10 386

(iii) Two WEAK triggers that also triggered BAT and had XRT data were also analysed. These are also termed as ‘candidate GRBs’.

Candidate triggers for our *Swift* ToO follow-up were selected with the requirement that at least one of the following criteria were met. First, triggers were chosen to be close to the 8σ STRONG threshold (our lowest was 6.7σ). This was to increase the chance of the trigger representing a real GRB. Trigger positions were also checked for high Galactic extinction and close proximity to nearby catalogued X-ray sources. Finally, triggers were generally only followed up if the trigger time coincided with the working hours of the on-call member of the *Swift* team. The criteria described above were not stringently adhered to for all triggers. We cannot claim that these triggers form a uniform or complete sample and biases towards high significance and lower Galactic column density are present. This was a pilot campaign aimed at determine whether real transient events exist among the WEAK trigger population and we stress that we do not make conclusions for the entire WEAK trigger population.

3 *SWIFT* ANALYSIS

The XRT and UVOT data from the 15 WEAK triggers with follow-up *Swift* observations discussed in Section 2.1 were analysed to determine the nature of the WEAK trigger events. The data were made available by the UK *Swift* Science Data Centre (UKSSDC; Evans et al. 2007, 2009).

Cleaned event files for our 11 ToOs were produced using the *Swift* XRT pipeline tool (v0.13.2). For the other four candidate GRBs, we used the existing XRT products made available by the UKSSDC. For each ToO a search for any sources with a probability of being due to statistical fluctuations <0.3 per cent (equivalent to 3σ) within the *INTEGRAL* error region (90 per cent confidence) was conducted using the sky image file. Source counts were derived from 30 arcsec radius regions centred on any detected X-ray source coordinates. Upper limits on non-detections were also obtained using Bayesian analysis described in Kraft, Burrows & Nousek (1991).

If a source was detected with the *Swift* XRT a further ToO observation was requested to identify whether the source was fading and thus could be confirmed as a GRB. If the source was detected again, and confirmed to be fading, a third observation was requested at a later date to check if the source had faded further. All positive detection coordinates were cross-referenced with the astrophysics catalogue data base Vizier[3] (Ochsenbein, Bauer & Marcout 2000) to identify any existing sources that could account for the X-ray emission. We obtained the following results:

(i) For 6 of the 15 WEAK triggers, comprising of two of our chosen ToOs and the four candidate GRBs, we had a detection with the XRT. The *Swift* XRT properties of these events, along with the non-detections, can be found in Table 2.

[3] http://vizier.u-strasbg.fr/viz-bin/VizieR

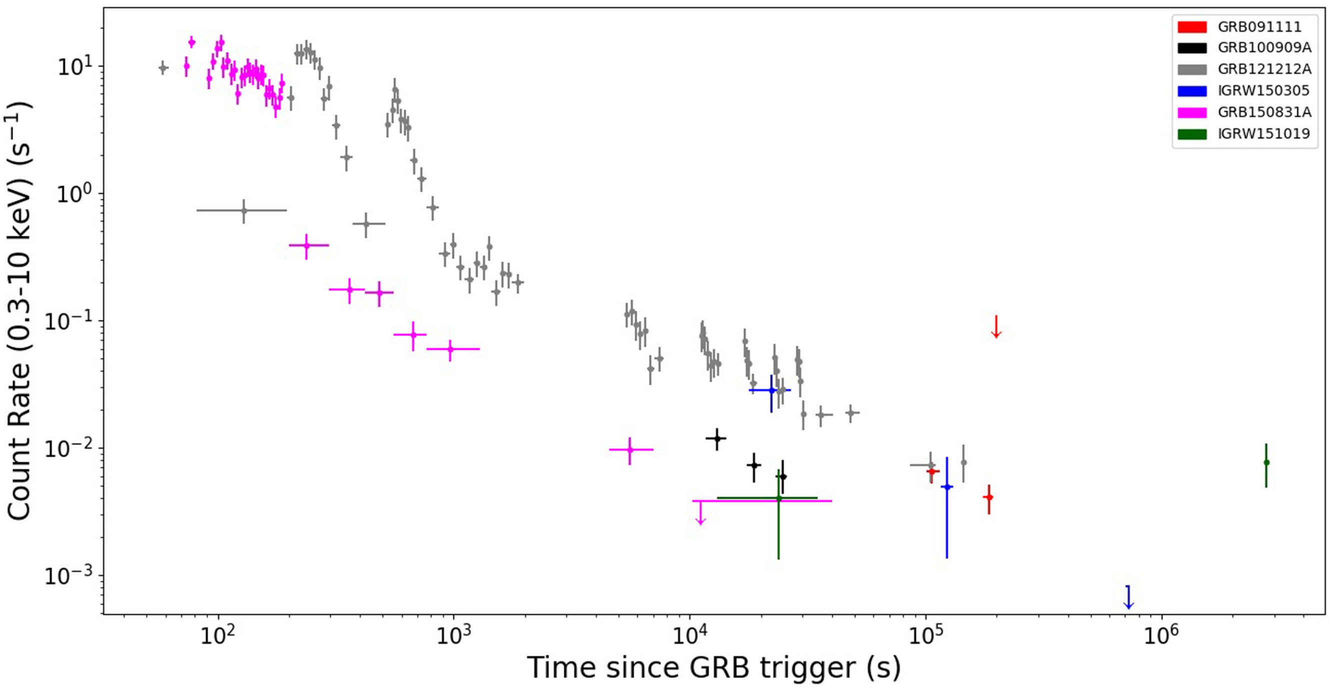

Figure 1. X-ray afterglows of the 6 WEAK *INTEGRAL* sources that were detected by *Swift* from our 15 WEAK triggers.

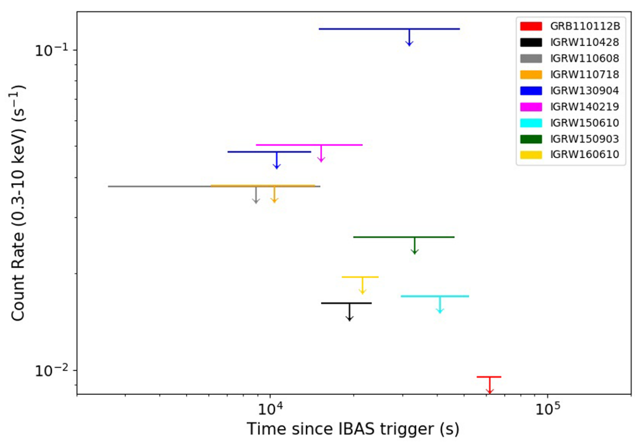

Figure 2. XRT 3σ Bayesian upper limits of the 9 non-detections out of our 15 selected WEAK triggers.

(ii) Subsequent observations found that five of these were fading X-ray sources, typical of a GRB afterglow (Costa et al. 1997; O'Brien et al. 2006) (see Fig. 1). The exception was IGRW 151019 (discussed in Section 3.2).

(iii) All six positive X-ray detections had no previously catalogued X-ray sources within 2 arcmin at the time of the observations. The XRT non-detection upper limits can be seen in Fig. 2.

Two of the candidate GRBs, GRB 121212A and GRB 150831A, were relatively well observed by the XRT (>10 data points) compared to the other WEAK trigger XRT sources as they also triggered BAT. These were further analysed to obtain both a spectral fit and X-ray afterglow decay slope. The results can be seen in Table 3 and Fig. 3 shows the spectrum for GRB 121212A. GRB 150831A has a $T_{90} \approx 2$ s – classifying it as a short GRB. Although ToO IGRW 110112 was an XRT non-detection at $6.2(\pm 0.6) \times 10^4$ s after the IBAS trigger, its initial gamma-ray trigger was seen simultaneously by *Fermi* Gamma-ray Burst Monitor (GBM; Connaughton 2011) and so was classified as a GRB. IGRW 110608, one of the non-detections appeared to have an unusually high and irregular X-ray background compared to the other ToOs. This may have reduced our chances of getting a detection.

In Fig. 4, we plot the time from the GRB to the start of the XRT observation ($T_{\rm START}$) against the weighted mean Galactic column density, $N_{\rm H}$(Gal) for both detections and non-detections. As the X-ray emission decays over time a later observation may result in a non-detection of an X-ray source that had been present at an earlier time. Additionally, high Galactic column density may reduce the chance of achieving a detection. The values for $N_{\rm H}$(Gal) were calculated using the method described in Willingale et al. (2013). Two sources observed less than 100 s after the initial trigger were both detected. Of the other 13 sources observed at later times after the triggers, 4 were detected and 9 were not. The column density and time since the trigger values for these detections and non-detections were similar and from our observations, we saw that the column density (up to $\approx 10^{22}$ cm^{-2}) and $T_{\rm START}$ (up to $\approx$70 000 s) had no significant impact as to whether a WEAK trigger would be detected by the XRT. However, we observed 15 sources only and two sources observed within 100 s of the trigger were both detected, so observing sources as promptly as possible would aid in detecting any potential afterglows.

For the six X-ray detections, we analysed the UVOT data to determine if any UV/optical sources were present. The data comprised one or more UVOT filters each with a number of separate images. Multiple images were aligned and summed up to create one image per exposure for each filter. If there were multiple exposures over all observations of the ToO these were also additionally summed together to create one image with the total exposure over all observations. It must be noted that the number of filters used during each ToO exposure was dependent upon those already designated to be used by *Swift* on the date of the observation (the image binning could vary per exposure so only 1×1 binned

Table 3. Table containing the X-ray spectral and afterglow light curve properties of WEAK GRBs with >10 binned data points. $N_{\rm H}$(Gal) is the fixed Galactic absorption column density and $N_{\rm H}$(Int) is the excess absorption. Spectral analysis was performed using XSPEC and fitting an absorbed power law where Γ is the photon index. The X-ray decay slopes were calculated using non-linear least squares fitting with various broken power-law models. For each case, a simple non-broken power law provided the best fit. All errors given at 90 per cent confidence level apart from the X-ray decay slopes – they are given at 1σ.

ToO name	$N_{\rm H}$(Gal) (10^{20} cm^{-2})	$N_{\rm H}$(Int) (10^{20} cm^{-2})	Γ	C-Stat (dof)	α
GRB 121212A	4.48	$21^{+0.5}_{-0.4}$	$2.24^{+0.14}_{-0.13}$	341 (369)	$-0.71^{+0.03}_{-0.03}$
GRB 150831A (WT)	11.4	$0^{+80.0}_{-0}$	$1.15^{+0.18}_{-0.1}$	322 (404)	$-2.67^{+0.22}_{-0.22}$
GRB 150831A (PC)	11.4	$0^{+18.0}_{-0}$	$1.53^{+0.28}_{-0.29}$	99 (93)	$-2.67^{+0.22}_{-0.22}$

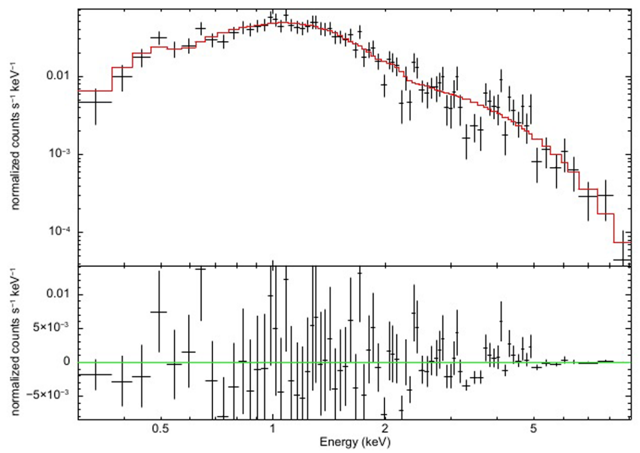

Figure 3. XRT spectrum of GRB 121212A with the best-fitting absorbed power-law model produced using XSPEC (red). The fit parameters can be seen in Table 3.

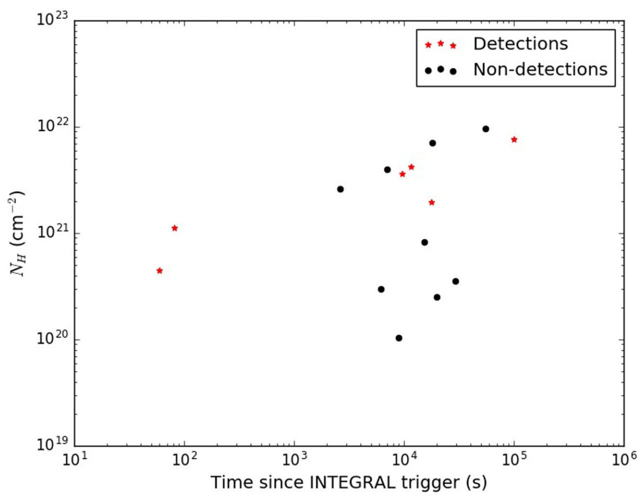

Figure 4. Plot of $T_{\rm START}$ against Galactic $N_{\rm H}$ of all of our 15 WEAK triggers including both XRT detections and non-detections.

images were used during the investigation – see *Swift* UVOT Online Manual).

To find the magnitude of a possible UVOT source, or upper limit on any non-detections, the *Swift* tool UVOTSOURCE was used with a significance of 3σ to distinguish between a possible source and non-detection upper limit (Breeveld et al. 2010). From our UVOT analysis we found:

(i) An optical source was marginally detected ($<5\sigma$) with the UVOT white filter coincident with the XRT position of GRB 121212A. A Vizier search of the source position revealed no reported optical source. The UVOT position of the GRB 121212A optical source was RA, Dec. (J2000) 177.79341, 78°.03780 with a 1σ positional error of 0.48 arcsec.

(ii) A marginal detection was also registered in the *v*, *b* and *u* bands for GRB 091111. Further analysis revealed that the event occurred within 30 arcsec of the centre of a very bright, saturated source that may have affected the background region near GRB 091111 resulting in a false detection.

(iii) A UV source detected with the m2 filter (9.2σ) was present very close to the 90 per cent XRT error circle of IGRW 151019 (see Section 3.2).

Table 4 contains the magnitudes and limits that were obtained for each source in each available filter. Some sources occurred in crowded fields affecting background subtraction. We also included Galactic reddening values for each source. The A_V values were taken from the Infrared Science Archive (IRSA)[4] using the method described in Schlafly & Finkbeiner (2011).

3.1 GRB 150305A

IGRW 150305 was confirmed to have a fading X-ray afterglow after requesting 3 ToOs over a time period of ≈8–9 d, the first of which began 17 ks after the WEAK trigger (see Fig. 5). A marginal detection was made in the white UVOT filter. A Vizier search of the GRB position revealed that no optical or X-ray catalogue matches for the XRT and UVOT positions.

The light curve of GRB 150305A was poorly sampled due to the limited exposure from the ToOs but it is consistent with a decay slope of $\alpha \approx 1$. An optimized fit could not be produced for the light curve so this decay slope is a rough estimation. Obtaining a spectrum is not possible due to the low number of counts detected: 102 in 6620 s. This was a detection of a new GRB directly from *Swift* follow-up of a WEAK trigger and was not identified elsewhere (Starling 2015).

3.2 IGRW 151019 – AGN candidate

IGRW 151019 had showed no signs of fading after four weeks; initially the count rate was $4.0(\pm 2.7) \times 10^{-3}$ s^{-1} increasing by a factor of ≈1–8 in the X-ray band over a time period of ≈1 month. There were only two observations of this source as a third ToO was not required as the source clearly was not fading. IGRW 151019 may

[4] http://irsa.ipac.caltech.edu/applications/DUST/

Table 4. UVOT multiband magnitudes (AB) and 3σ upper limits of the six XRT detected sources. Filters ordered with decreasing wavelength.

Name	White	v	b	u	$w1$	$m2$	$w2$	Source?	A_V (mag)
IGRW 151019	–	–	–	–	>21.75	22.16(±0.15)	–	Yes	0.75
GRB 150831A	>21.54	>19.82	>19.90	>21.34	>21.85	>22.39	>23.10	No	0.30
GRB 150305A	-	–	–	–	>22.68	>22.74	–	No	0.45
GRB 121212A	23.89(±0.38)	>20.22	>20.75	>22.07	>23.00	>22.73	>22.95	No	0.18
GRB 100909A	>22.52	>20.07	>21.26	>21.78	>21.73	>22.19	>21.99	No	1.37
GRB 091111	–	19.48(±0.24)[a]	18.92(±0.28)[a]	21.76(±0.23)[a]	>21.94	>22.35	>22.32	No	4.79

Note. [a]The GRB 091111 XRT position was within 10 arcsec of a very bright, saturated source and further analysis of the images suggest that the detections in the v, b and u filters are probably not real.

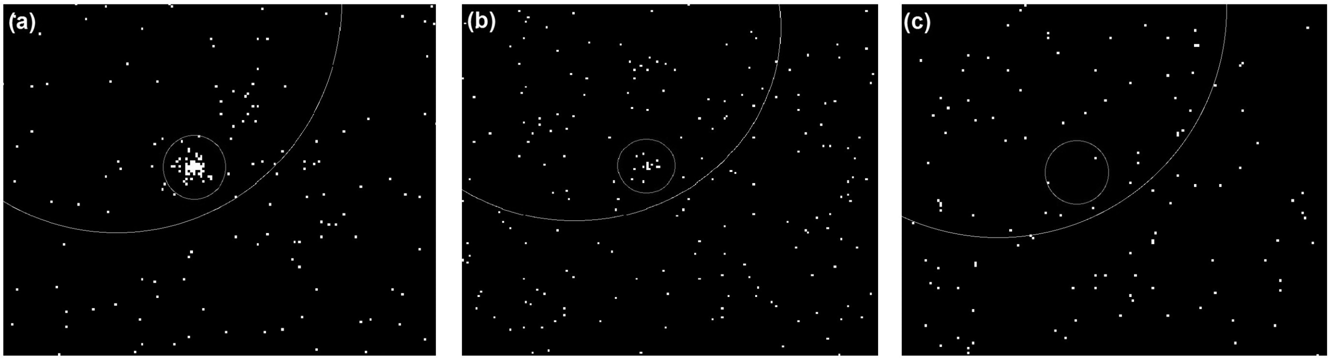

Figure 5. Images showing the X-ray source IGRW 150305/GRB 150305A (cyan) within the *INTEGRAL* error circle (yellow). The images correspond to observation times of (1.7–2.7) × 10^4 s (a), (1.2–1.3) × 10^5 s (b) and (7.0–7.4) × 10^5 s (c) after the GRB occurred with XRT exposure times of 3.0 ks (a), 3.7 ks (b) and 2.4 ks (c), respectively. The point source clearly fades over time and is undetectable after ≈7.4 × 10^5 s (8–9 d).

therefore not be a GRB but a steady source. Analysis of the spectrum when fitted with an absorbed power law gave a total column density, $N_{\rm H} = 4.0^{+5.0}_{-3.0} \times 10^{21}$ cm^{-2} and a photon index, $\Gamma = 1.71 \pm 0.37$, which is broadly consistent with that of an AGN (Nandra & Pounds 1994; Tozzi et al. 2006; Brightman & Nandra 2011).

Inside the *Swift* XRT error circle lies the catalogued AllWISE source J193108.05+310756.4 (Cutri & et al. 2014). The source is within 1.8 arcsec of the centre of the XRT position and within the 90 per cent XRT error region. The UVOT source we detected (Table 4) for IGRW 151019 in the m2 filter has is RA, Dec. (J2000) 292.78334, 31°.13252 with a 1σ positional error of 0.49 arcsec. A catalogued *Gaia* source has a position coincident to the UVOT source to within 0.5 arcsec. However, these sources lie just outside the 90 per cent XRT error region so we cannot confirm their association with the new X-ray transient. In addition, the Galactic extinction in this direction, $A_V \approx 0.75$. Examining the *WISE* source in more depth, we find that its *WISE* colours, $W1 - W2 = 0.8$ and $W2 - W3 = 2.4$, are consistent with that of an AGN (Mingo et al. 2016). It is possible that a transient event may have caused the initial *INTEGRAL* WEAK trigger and the steady source may simply be a chance coincidence observation. However, this is unlikely and we conclude that IGRW 151019 is likely an AGN.

4 IBAS AND *SWIFT* GRB SAMPLE PROPERTIES

In Section 1, we discussed that a low-luminosity GRB population could exist and that *INTEGRAL* may be capable of detecting it. Including the WEAK alert GRBs, we have confirmed, the IBAS GRB sample size currently stands at 114. The *Swift* sample size stands at 1060 GRBs with XRT detections for 846 GRBs (all values correct as of 2016 July 1 and *Swift* numbers were taken from the *Swift* GRB Table[5]).

Fig. 6 shows the T_{90} and peak flux distributions of the *INTEGRAL* IBAS and *Swift* BAT samples. Analysis shows that the IBAS sample has a lower mean T_{90} (47 s compared to 70 s). However, the *Swift* sample has a higher percentage of short GRBs compared to IBAS; 95 short GRBs out of the 992 *Swift* GRBs with measured T_{90} (9.6 per cent) compared to 6 short GRBs out of 114 *INTEGRAL* GRBs (5.3 per cent). The mean peak flux of the IBAS GRB sample is also lower than that of the *Swift* sample (2.0 ph cm^{-2} s^{-1} compared to 3.6 ph cm^{-2} s^{-1}) meaning *INTEGRAL* routinely reaches lower peak flux values as a proportion of the total sample. With a lower average T_{90} and peak flux it is more likely that the fluence distribution of *INTEGRAL* may be skewed towards fainter GRBs than *Swift* and with the addition of the lower IBIS sensitivity (discussed in Section 1) *INTEGRAL* may be better suited to probing this lower luminosity GRB population.

4.1 Can IBAS be used to probe low-fluence GRBs?

Our IBAS GRB sample contains 92 of the 114 IBAS GRBs, i.e. all those that have calculated fluence values. All IBAS T_{90} values were taken from the IBAS webpage[1] but did not have any associated error limits. The IBAS GRB fluxes were calculated in XSPEC using a simple power-law/cut-off model. The flux values were then multiplied by the T_{90} values to calculate the fluences. Several fluence values were taken from Vianello et al. (2009) and Bošnjak et al. (2014) and the properties of all IBAS GRBs with published and estimated measurements can be found in Table A1 .

[5] http://swift.gsfc.nasa.gov/archive/grb_table/

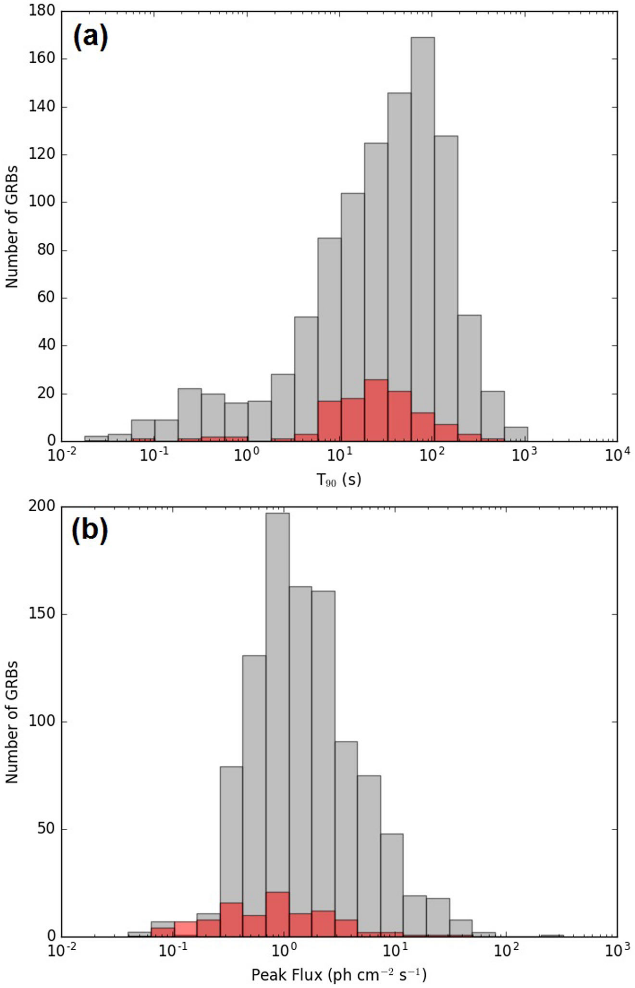

Figure 6. Histograms of T_{90} and peak flux distributions of both the *Swift* BAT (light grey) and IBAS (red) GRB samples. The peak flux values are measured between 15–150 keV for *Swift* and 20–200 keV for *INTEGRAL*. The fraction of short GRBs in the *Swift* and IBAS samples are 9.6 per cent and 5.3 per cent, respectively.

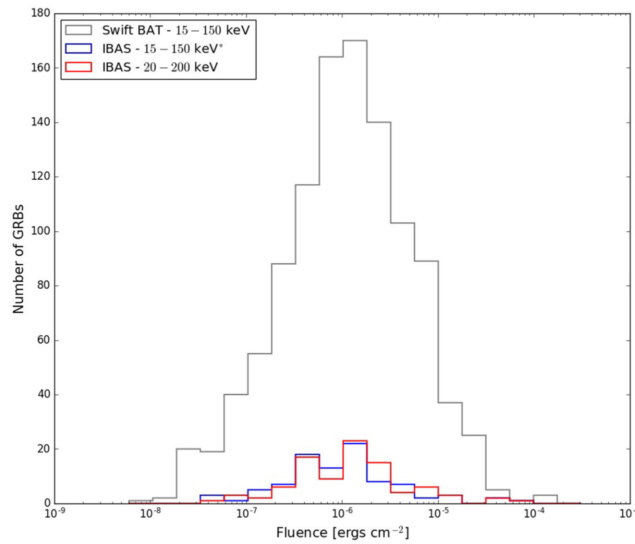

Figure 7. Fluence distributions of both the *Swift* BAT and the IBAS GRB samples. *Calculated using method described in Section 4.1.

For the IBAS GRBs detected by the XRT, we calculated the X-ray flux values at 11 h by fitting a series of single/broken power laws to the *Swift* X-ray afterglow light curves and performing an f-test to determine the best-fitting model. Once the best-fitting model was obtained this was extrapolated to 39 600 s (11 h) and an estimate for the X-ray flux was determined. For the 1026 *Swift* GRBs with fluences, both the fluence, associated errors (at 90 per cent confidence) and X-ray flux at 11 h values were taken from the NASA Goddard Space Flight Center *Swift* GRB Table[1]. X-ray flux values $< 10^{-14}$ erg cm^{-2} s^{-1} were omitted as they were deemed too faint for *Swift* to detect and are therefore non-physical measurements. This resulted in 824 *Swift* GRBs and 33 IBAS GRBs with calculated X-ray flux values. It must be noted that the *Swift* GRB fluences are measured in the energy range of 15–150 keV, whereas the *INTEGRAL* GRB fluences are measured between 20–200 keV. We found that the flux, and therefore, fluence ratios between these two energy bands was $\frac{f_{20-200}}{f_{15-150}} \approx 1.22$ when measured from spectral fits for a small number of typical sources from our sample. We highlight that this is a mean ratio used to give an indication of the IBAS fluence values in the BAT energy band and will vary between GRBs within the sample. We also note that the T_{90} can vary between different energy bands but we assumed that it remains constant for this conversion. Fig. 7 shows the Swift GRB fluence distribution overlaid with the IBAS GRB fluence distribution in both the 20–200 keV and 15–150 keV energy bands.

To determine if the IBAS and *Swift* GRB sample fluence distributions came from the same underlying population, a K-S test was performed on the *Swift* and IBAS fluence values in their respective 15–150 and 20–200 keV energy bands. If the test rejected the null hypothesis; that the underlying distribution of the samples was the same at a 95 per cent confidence level ($p < 0.05$) then it was assumed that the samples were not part of the same underlying distribution. The K-S test returned a p-value of 0.37 for the fluence distribution so we cannot reject the null hypothesis and we conclude that the *INTEGRAL* IBAS and *Swift* GRB samples most likely belong to the same distribution. Moreover, the mean fluence values are similar, 3.66×10^{-6} and 3.94×10^{-6} erg cm^{-2} for the *Swift* and IBAS samples, respectively. Converting the IBAS fluence values into the 15–150 keV band using the ratio calculated previously gives a mean fluence value of 3.23×10^{-6} erg cm^{-2} and when compared to the *Swift* distribution gives a K-S p-value of 0.06. This results in the same conclusion as before; the two distributions most probably belong to the same fluence distribution.

We also analysed the correlations between GRB fluence, T_{90} and X-ray flux at 11 h for both the IBAS and *Swift* GRB samples. The Spearman rank coefficients for fluence – T_{90} were 0.52($\pm$0.07) and 0.66($\pm$0.02) corresponding to p-values of 5.7×10^{-8} and 3.8×10^{-130} for the IBAS and *Swift* samples, respectively. The Spearman rank coefficients for fluence – X-ray flux were 0.65($\pm$0.11) and 0.61($\pm$0.02) corresponding to p-values of 2.4×10^{-5} and 3.96×10^{-90} for the IBAS and *Swift* samples, respectively. These values show these parameters exhibit significant correlation. Similar correlations have been reported in previous investigations (Gehrels et al. 2008; Evans et al. 2009; Margutti et al. 2013; Grupe et al. 2013). These authors acknowledge a wide spread in the data (to within an order of magnitude) due to a range of factors. We do not have available errors for the IBAS T_{90} values and these can be underestimated for very long GRBs. Our extrapolation values of X-ray flux at 11 h do not have any associated errors and for some GRBs can only be taken as rough estimates due to the low

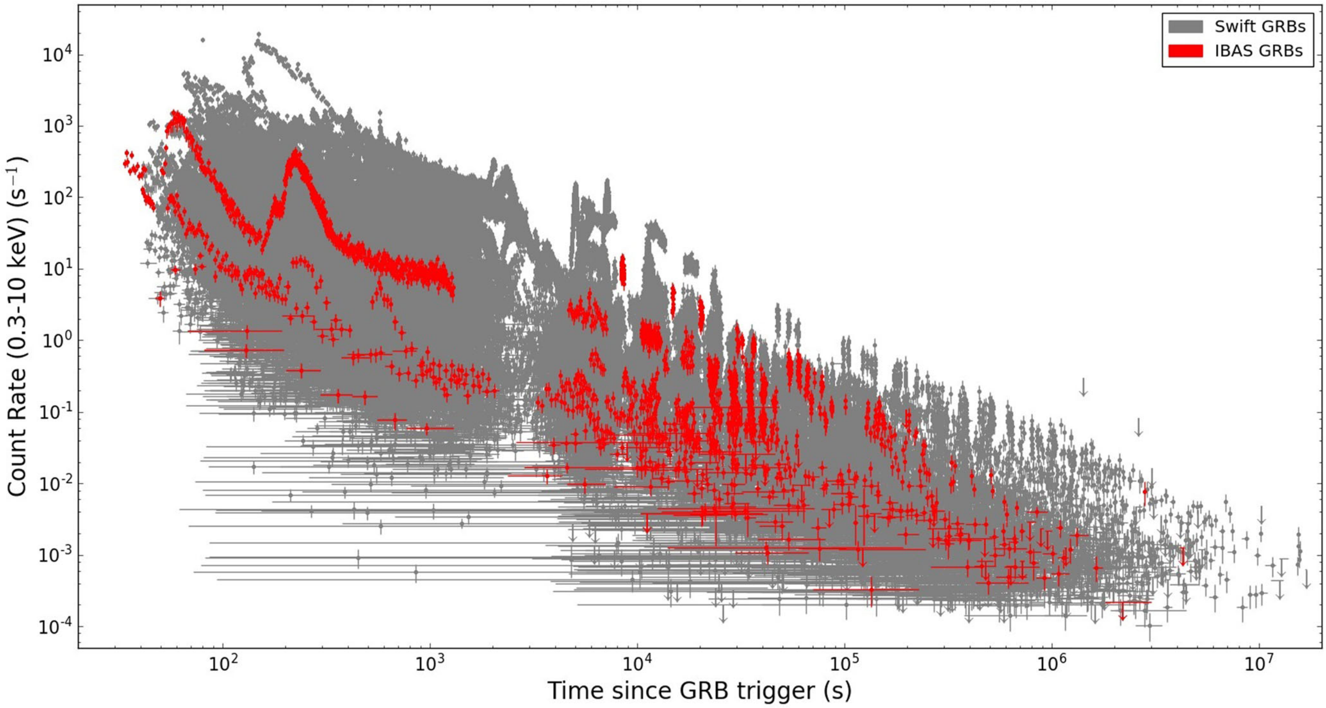

Figure 8. X-ray afterglows of the *Swift* GRB sample and the 54 IBAS GRBs observed by *Swift*/XRT.

number of data bins. Additionally, we have used the observed X-ray flux, prior to correction for line-of-sight absorption. Although we have not fully accounted for these effects our correlations are significant. We conclude that our correlations agree with similar correlations from previous investigations.

Fig. 8 shows the X-ray afterglows of the IBAS and *Swift* GRB samples. The plot highlights that the X-ray afterglow distribution of the IBAS sample sits comfortably within the *Swift* X-ray GRB afterglow distribution. The mean X-ray flux values at 11 h for the IBAS and *Swift* samples are 2.85×10^{-12} and 1.48×10^{-12} erg cm^{-2} s^{-1} showing that, on average, the X-ray flux of the *Swift* sample GRBs is lower. However, only 54 IBAS GRBs were detected by the XRT; not all were followed up, some were non-detections, and only 33 were sufficiently sampled to obtain a value of X-ray flux at 11 h.

Swift and *INTEGRAL* regularly detect similar fluence GRBs; however, the *Swift* sample has a low fluence, short GRB tail that the IBAS sample does not. *Swift* has also detected six GRBs which may belong to a further subclass of 'ultralong' GRBs where T_{90} values $\gtrsim$ 1000 s (Gendre et al. 2013; Virgili et al. 2013; Evans et al. 2014; Levan et al. 2014; Cucchiara et al. 2015). However, with this low number of 'ultralong' GRBs (<1 per cent of the sample), we do not expect to have detected any with IBAS. *Swift* has detected ≈10 times the number of GRBs than IBAS has detected. With such a large *Swift* sample you would expect to see some very faint and very long GRBs and the differences in the distributions may arise from the smaller IBAS sample size and low number statistics. From this investigation, we conclude that the *Swift* and IBAS GRB distributions are similar but not identical.

5 CONCLUSIONS

We investigated 15 *INTEGRAL* WEAK triggers utilizing *Swift* for follow-up observations. Among these WEAK triggers, we confirm seven astrophysical events – six GRBs and one candidate AGN. IGRW 150305 found directly from one of our chosen ToOs was identified as a GRB through this ToO campaign alone.

Comparisons of the fluence distributions of the full IBAS and *Swift* GRB samples showed that the two are similar but not identical. We also confirm correlations between the gamma-ray and X-ray properties found in previous investigations for both samples. Both the IBAS GRB fluence and X-ray afterglow light curve distributions comfortably lie within the *Swift* distributions. We conclude that *Swift* and IBAS typically reach similar fluence limits, while *Swift* appears to be more sensitive to short, low fluence GRBs.

We only sample ≈4 per cent of the total WEAK trigger population. Hence, we do not make any statistical statements for the total sample. We have shown that *INTEGRAL* can detect real GRB events below the STRONG threshold, along with other high-energy transients and variables such as AGN. This allows future work to uncover the nature of yet more WEAK triggers to determine whether *INTEGRAL* can detect fainter GRBs.

ACKNOWLEDGEMENTS

The research leading to these results has received funding from the European Union's Horizon 2020 Programme under AHEAD project (grant agreement n. 654215). ABH is supported by an Science and Technology Facilities Council (STFC) studentship. R. L. C. Starling and K Wiersema acknowledge support from STFC. This work made use of data supplied by the UKSSDC at the University of Leicester, which is supported by the UK Space Agency. S. Mereghetti acknowledges the support of ASI/INAF agreement No. 2016-025-R.0. We also thank the referee for useful comments and feedback. DG acknowledges the financial support of the UnivEarthS Labex program at Sorbonne Paris Cité (ANR-10-LABX-0023 and ANR-11-IDEX-0005-02). This research has made use of the VizieR

catalogue access tool, CDS, Strasbourg, France. The original description of the VizieR service was published in A&AS 143, 23.

During the reviewing process for this paper, our colleague Neil Gehrels passed away. We would like to acknowledge not only his input into this work, but his immense contributions to high-energy astrophysics as a whole.

REFERENCES

Barthelmy S. D., 2004, in Flanagan K. A., Siegmund O. H. W., eds, Proc. SPIE Conf. Ser. Vol. 5165, , X-Ray and Gamma-Ray Instrumentation for Astronomy XIII. SPIE, Bellingham, p. 175
Bird A. J. et al., 2016, ApJS, 223, 15
Bošnjak Ž., Götz D., Bouchet L., Schanne S., Cordier B., 2014, A&A, 561, A25
Breeveld A. A. et al., 2010, MNRAS, 406, 1687
Brightman M., Nandra K., 2011, MNRAS, 413, 1206
Burrows D. N. et al., 2005, Space Sci. Rev., 120, 165
Chapman R., Tanvir N. R., Priddey R. S., Levan A. J., 2007, MNRAS, 382, L21
Cline T. L. et al., 1999, A&AS, 138, 557
Connaughton V., 2011, GRB Coordinates Network, 11569
Costa E. et al., 1997, Nature, 387, 783
Courvoisier T. J.-L. et al., 2003, A&A, 411, L53
Cucchiara A. et al., 2015, ApJ, 812, 122
Cutri R. M. et al., 2014, VizieR Online Data Catalog, 2328
Daigne F., Mochkovitch R., 2007, A&A, 465, 1
Evans P. A. et al., 2007, A&A, 469, 379
Evans P. A. et al., 2009, MNRAS, 397, 1177
Evans P. A. et al., 2014, MNRAS, 444, 250
Foley S., McGlynn S., Hanlon L., McBreen S., McBreen B., 2008, A&A, 484, 143
Gehrels N., Mészáros P., 2012, Science, 337, 932
Gehrels N. et al., 2004, ApJ, 611, 1005
Gehrels N. et al., 2008, ApJ, 689, 1161
Gendre B. et al., 2013, ApJ, 766, 30
Götz D., 2013, preprint (arXiv:1302.4847)
Gotz D., Mereghetti S., Bozzo E., Ferrigno C., Pavan L., Borkowski J., 2016, GRB Coordinates Network, 19621
Grupe D., Nousek J. A., Veres P., Zhang B.-B., Gehrels N., 2013, ApJS, 209, 20
Kouveliotou C., Meegan C. A., Fishman G. J., Bhat N. P., Briggs M. S., Koshut T. M., Paciesas W. S., Pendleton G. N., 1993, ApJ, 413, L101
Kraft R. P., Burrows D. N., Nousek J. A., 1991, ApJ, 374, 344
Lebrun F. et al., 2003, A&A, 411, L141
Levan A. J. et al., 2014, ApJ, 781, 13
Liang E., Zhang B., Virgili F., Dai Z. G., 2007, ApJ, 662, 1111
Margutti R. et al., 2013, MNRAS, 428, 729
Mereghetti S., Götz D., Borkowski J., Walter R., Pedersen H., 2003, A&A, 411, L291
Mereghetti S., Gotz D., Ferrigno C., Bozzo E., Ducci L., Borkowski J., 2015a, GRB Coordinates Network, 18210
Mereghetti S., Gotz D., Ferrigno C., Bozzo E., Saral G., Borkowski J., 2015b, GRB Coordinates Network, 18623
Mereghetti S., Gotz D., Ferrigno C., Bozzo E., Favre T., Borkowski J., 2016, GRB Coordinates Network, 19046
Mészáros P., Rees M. J., 1997, ApJ, 476, 232
Mingo B. et al., 2016, MNRAS, 462, 2631
Nandra K., Pounds K. A., 1994, MNRAS, 268, 405
Norris J. P., 2002, ApJ, 579, 386
Norris J. P., Bonnell J. T., Kazanas D., Scargle J. D., Hakkila J., Giblin T. W., 2005, ApJ, 627, 324
O'Brien P. T. et al., 2006, ApJ, 647, 1213
Ochsenbein F., Bauer P., Marcout J., 2000, A&AS, 143, 23
Pescalli A. et al., 2016, A&A, 587, A40
Piran T., 2003, Nature, 422, 268
Roming P. W. A. et al., 2005, Space Sci. Rev., 120, 95
Sazonov S. Y., Lutovinov A. A., Sunyaev R. A., 2004, Nature, 430, 646
Schlafly E. F., Finkbeiner D. P., 2011, ApJ, 737, 103
Soderberg A. M. et al., 2004, Nature, 430, 648
Starling R., 2015, GRB Coordinates Network, 17551
Tozzi P. et al., 2006, A&A, 451, 457
Ubertini P. et al., 2003, A&A, 411, L131
Vedrenne G. et al., 2003, A&A, 411, L63
Vianello G., Götz D., Mereghetti S., 2009, A&A, 495, 1005
Virgili F. J. et al., 2013, ApJ, 778, 54
von Kienlin A. et al., 2003, A&A, 411, L299
Wijers R. A. M. J., Rees M. J., Meszaros P., 1997, MNRAS, 288, L51
Willingale R., Starling R. L. C., Beardmore A. P., Tanvir N. R., O'Brien P. T., 2013, MNRAS, 431, 394
Winkler C. et al., 2003, A&A, 411, L1
Woosley S. E., Heger A., 2006, ApJ, 637, 914

APPENDIX A: SUPPLEMENTARY MATERIAL CONTAINING IBAS GRB GAMMA-RAY AND X-RAY DATA USED DURING THIS INVESTIGATION

Table A1. The prompt emission fluence, T_{90} and X-ray afterglow flux of all 92 IBAS GRBs within our sample. All T_{90} values were taken from IBAS[1]. Some GRBs were not observed by *Swift* or had very poorly sampled *Swift* XRT afterglows and therefore an X-ray flux at 11 h could not be obtained. Some fluence values contain no errors as the fitted model would not converge and would not provide an error on the normalization. This meant no error could be found on the flux values and therefore the fluence values but the values should still be representative of the actual fluence. Fluence values for GRB 150831, GRB 151120A, GRB 160221A and GRB 160629A are approximations from the GCN Circulars (Mereghetti et al. 2015a,b, 2016; Gotz et al. 2016) as the spectral data were not yet public.

Name	Fluence (20–200 keV) (10^{-7} erg cm^{-2})	X-ray flux at 11 h (0.3–10 keV) (10^{-12} erg cm^{-2} s^{-1})	T_{90} (s)
GRB 030227*	$6.10^{+3.50}_{-5.90}$	–	15
GRB 030320*	$54.2^{+13.3}_{-11.7}$	–	48
GRB 030501*	$17.2^{+1.60}_{-3.10}$	–	25
GRB 030529#	0.52	–	16
GRB 031203*	$10.6^{+2.70}_{-3.00}$	–	19
GRB 040106*	$95.0^{+23.0}_{-30.0}$	–	47
GRB 040223*	$27.2^{+0.80}_{-1.90}$	–	258
GRB 040323*	$20.6^{+2.30}_{-2.90}$	–	14
GRB 040403*	$4.00^{+1.60}_{-3.70}$	–	15
GRB 040422*	$4.90^{+1.00}_{-3.60}$	–	10
GRB 040624#	4.81	–	27
GRB 040730*	$6.30^{+4.40}_{-3.30}$	–	42
GRB 040812#	1.40	–	8
GRB 040827*	$11.1^{+2.80}_{-4.00}$	–	32
GRB 040903#	0.96	–	7
GRB 041015#	5.12	–	30
GRB 041218*	$58.2^{+3.50}_{-3.70}$	–	38
GRB 041219A*	$867^{+0.50}_{-129}$	–	239
GRB 050129#	4.10	–	30
GRB 050223	$10.8^{+2.70}_{-2.10}$	0.19	30
GRB 050502A*	$13.9^{+1.10}_{-4.00}$	–	>11

Table A1 – *continued*

Name	Fluence (20–200 keV) (10^{-7} erg cm^{-2})	X-ray flux at 11 h (0.3–10 keV) (10^{-12} erg cm^{-2} s^{-1})	T_{90} (s)
GRB 050504*	$10.0^{+4.10}_{-4.50}$	–	44
GRB 050520*	$16.6^{+4.90}_{-5.00}$	0.20	52
GRB 050522#	0.69	–	11
GRB 050525A*	$154^{+5.70}_{-8.40}$	1.5	9
GRB 050626*	$6.30^{+0.40}_{-1.00}$	–	52
GRB 050714A	$5.58^{+2.75}_{-1.84}$	–	34
GRB 050918*	$30.2^{+10.5}_{-9.0}$	–	280
GRB 050922A#	0.59	–	10
GRB 051105B*	$2.80^{+1.50}_{-2.00}$	-	14
GRB 051211B*	$16.1^{+4.60}_{-3.30}$	0.92	47
GRB 060114*	$16.0^{+4.60}_{-3.30}$	—	80
GRB 060130#	2.25	—	19
GRB 060204A*	$4.80^{+2.40}_{-3.30}$	–	52
GRB 060428C*	$18.6^{+2.20}_{-3.90}$	–	10
GRB 060901*	$62.2^{+3.50}_{-5.90}$	1.2	16
GRB 060930#	2.63	–	9
GRB 060912B*	$12.0^{+5.80}_{-5.10}$	–	140
GRB 061025*	$10.1^{+1.30}_{-4.80}$	0.14	11
GRB 061122*	$155^{+3.40}_{-5.30}$	2.2	12
GRB 070309	$4.93^{+3.12}_{-1.98}$	–	22
GRB 070311*	$23.6^{+1.70}_{-5.30}$	1.22	32
GRB 070615	2.01	–	15
GRB 070707	$3.58^{+4.04}_{-1.94}$	–	0.7
GRB 070925*	$36.1^{+1.70}_{-3.40}$	–	19
GRB 071003	$94.6^{+4.22}_{-2.96}$	3.5	38
GRB 071109*	$3.60^{+4.00}_{-3.50}$	–	30
GRB 080120	$13.2^{+17.0}_{-7.67}$	0.13	15
GRB 080603A	$12.3^{+1.70}_{-5.90}$	1.5	150
GRB 080613A*	$12.3^{+1.70}_{-5.90}$	–	30
GRB 080723B*	$396^{+6.70}_{-6.70}$	12.6	95
GRB 080922*	$17.3^{+6.90}_{-6.50}$	–	60
GRB 081003B*	$26.2^{+2.00}_{-24.5}$	–	20
GRB 081016*	$22.0^{+1.40}_{-4.50}$	–	30
GRB 081204*	$5.10^{+5.10}_{-4.80}$	–	12
GRB 090107B*	$12.4^{+1.30}_{-4.60}$	0.73	15
GRB 090625B*	$12.4^{+1.20}_{-2.00}$	0.38	8
GRB 090702	$1.93^{+1.44}_{-0.81}$	–	6
GRB 090704*	$54.0^{+4.90}_{-8.00}$	–	70
GRB 090814B*	$15.1^{+2.30}_{-2.40}$	1.4	42
GRB 090817*	$18.7^{+10.9}_{-9.80}$	2.4	30
GRB 091111	$20.0^{+5.90}_{-0.82}$	–	100
GRB 091202	$7.03^{+3.02}_{-2.35}$	–	25
GRB 091230	$17.9^{+20.5}_{-9.57}$	–	70
GRB 100103A*	$52.5^{+2.10}_{-4.00}$	2.1	30
GRB 100518A*	$5.20^{+4.40}_{-3.80}$	0.87	25
GRB 100713A	$5.65^{+2.65}_{-1.80}$	0.20	20
GRB 100909A	$21.5^{+7.00}_{-4.70}$	0.26	60
GRB 101112A*	$21.1^{+4.40}_{-7.40}$	0.50	6
GRB 110206A	$17.2^{+11.6}_{-6.10}$	2.0	15
GRB 110708A*	$24.8^{+1.90}_{-4.60}$	–	50
GRB 110903A*	$148^{+11.9}_{-17.5}$	3.8	430
GRB 120202A	$8.00^{+2.10}_{-7.70}$	–	70
GRB 120419A	$3.88^{+6.18}_{-2.49}$	–	15
GRB 120711A	$440^{+50.0}_{-5.00}$	40	135
GRB 121102A	$24.1^{+12.4}_{-8.10}$	0.56	25
GRB 121212A	1.50	0.46	10
GRB 130513A	$17.0^{+10.3}_{-6.50}$	–	50
GRB 130514B	$10.2^{+14.4}_{-6.20}$	1.6	10
GRB 130903A	$17.1^{+8.10}_{-5.40}$	–	70
GRB 131122A	$24.8^{+12.3}_{-8.20}$	–	80
GRB 140206A	$16.0^{+3.00}_{-3.00}$	9.2	>60
GRB 140320B	$12.7^{+11.8}_{-5.94}$	0.55	100
GRB 140320C	3.52	–	30
GRB 140815A	$5.00^{+5.10}_{-2.59}$	–	8
GRB 141004A	$6.92^{+6.88}_{-3.40}$	0.09	4
GRB 150219A	$57.1^{+14.9}_{-11.2}$	0.62	60
GRB 150305A	$12.1^{+14.2}_{-6.45}$	–	100
GRB 150831A	≈3	0.33	2
GRB 151120A	≈20	0.66	50
GRB 160221A	≈5	–	10
GRB 160629A	≈60	–	100

Notes. *Fluence values taken from Bošnjak et al. (2014).
#Fluence values taken from Vianello et al. (2009).

This paper has been typeset from a TEX/LATEX file prepared by the author.